

Fraud Detection over Ethereum Blockchain

CST4340 – COURSEWORK 2

Huma Zafar M00899071

Contents

1. Introduction	2
2. Research Objectives	2
3. Methodology	3
3.1 Dataset	3
3.2 Data Pre-Processing	3
3.3 Data Visualisation	4
3.4 Data Mining Tasks	10
4. Conclusion	22
5. Appendix A – Workflow Diagrams.....	23
6. References.....	35

1. Introduction

As early as 2013, Vitalik Buterin introduced Ethereum with the possibility of its widespread use (Antonopoulos, 2018). There are several applications based on the Ethereum protocol, including ERC-20 tokens, which are Ethereum-based tokens that can be created and deployed on the Ethereum network. Over 400 million transactions have been made on Ethereum since its inception. There have been a number of illegal activities related to Ethereum, including smart-Ponzi schemes, phishing, money laundering, and fraud. Detecting and predicting such attacks over blockchain can be achieved through anomaly detection for blockchain.

The paper makes a number of contributions; first of all, it proposes a Random Forest Classifier, which is an effective method for detecting illicit accounts on the Ethereum network based on the testing of 8 models of four distinct types (Decision Tree, Random Forest, Gradient Boosting, and Extreme Gradient Boosting); secondly, it gives a multiple linear regression model for estimating total Ethereum transfers; and thirdly, it provides coherent and graphical representations of historical data. The software tool, KNIME is used to execute the statistical tasks. This tool uses visual nodes to do descriptive, predictive and prescriptive analytics (Berthold et al., 2009).

2. Research Objectives

This paper is designed to identify fraudulent transactions on the Ethereum Blockchain using the most effective classification model possible. It seeks to find illegitimate transactions using the best-fit model selected from four classification models: decision trees, random forests, gradient boost and extreme gradient boost models. Additionally, it investigates the possibility of calculating the total amount of Ether that a wallet has received and transferred. To determine which models are well-fitted, it performs statistical tests for model fitness. A visual display of token transaction history is another goal. Ultimately, it aims to assess the internal validity, external validity, and reliability of the finalised models.

3. Methodology

3.1 Dataset

Ethereum dataset was downloaded from Kaggle, a platform for data science. Wallet addresses used in transactions are classified as fraud by the Ethereum community for illicit behavior, such as imitating other contract addresses, operating fake lotteries, conducting fake initial coin offerings (ICOs), impersonating other users, operating Ponzi schemes, phishing, and mirroring websites. In this case, it is assumed that the dataset consists of supervised information and that no time-dependent effects exist. An overview of the dataset is provided in Table 1.

Table 1. Normal transaction fields of interest.

Field of Interest	Description	Data Type
Flag	Determines whether account is flagged for fraudulent activity	Boolean (1 = Fraud, 0= Fair)
Address	Wallet Address on Ethereum Blockchain	String
ERC20 most sent token type	Name of ERC20 token used for transfer of fund	String
ERC20_most_rec_token_type	Name of ERC20 token used for transfer of fund	String
Sent tnx	Number of Transaction taken placed for the transfer of fund	Integer
Received Tnx	Number of Transaction taken placed to receive the fund	Integer
total Ether sent	Total Amount Transferred (ether)	Float
total ether received	Total Amount Received (ether)	Float

3.2 Data Pre-Processing

From the original dataset of 12,147 rows, 2,022 rows were randomly selected. The columns and rows of the data are manually selected as part of the data reduction process. There are 34 columns in the file, out of which 8 have been extracted. As shown in Table 1, the selected column and row type are described. Wallet addresses on the Ethereum Blockchain are generated as unique addresses (Antonopoulos, 2018), so duplicate addresses have been removed. A subsequent deletion was made of the columns containing 'none' and blank rows. The final row count was 1075 after filtering out non-unique accounts through the data cleansing process. Appendix A, Figure 2, illustrates the pre-processing technique workflow on KNIME.

The data mining process was applied to two different sets of data from the same dataset. In the first set, 272 unique tokens were transferred and 340 unique tokens were received in 1075

wallet addresses. This dataset is called dataset A. Subsequently, on KNIME (see Figure 11, 12, 13 and 14 on Appendix A), the second analysis was conducted after the data transformation had been completed, while categorizing the aggregate 612 tokens into 8 categories: EOS, OmiseGO, Ether, Golem, TheDAO, DATAcoin, DMTS, and others; this one is named as dataset B. With 612 tokens, graphical explanations of data became difficult. Hence, the tokens are reclassified into 8 categories based on overall transaction volume, and Ethereum is included as well since it forms the first layer of all ERC20 tokens.

3.3 Data Visualisation

It is evident from the data sample selected that fraudulent activities are substantially more prevalent than fair transactions, as shown in Figure 1 and Figure 2. This indicates sampling bias in the extraction of data from the Ethereum Blockchain's general population. This section aims to provide an overview of the past trends in token transactions in terms of fair and fraudulent transactions. For this descriptive analysis, the histograms, donut pie charts, and linear correlations are used to visualize the data. Histogram is chosen because they provide a clear retrospective analysis of ERC20 token transactions. Pie charts illustrate the overall classification of flagged and fair transactions. These charts facilitate the identification of relationships and findings that are not readily apparent in raw data. All of these graphical representations are aimed at comprehending current data and how it can be used to generate new models. All the donut pies are in two colours: blue and orange. Blue is for fair transaction. Contrarily, orange is for fraud transaction.

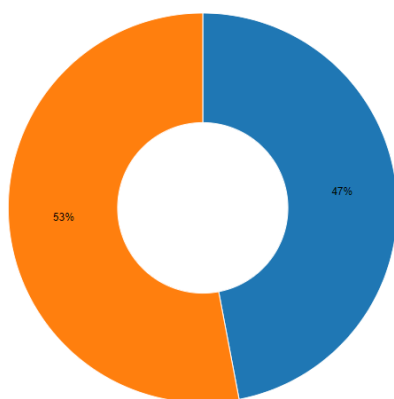


Figure 1: Donut pie chart for Overall total ether transferred

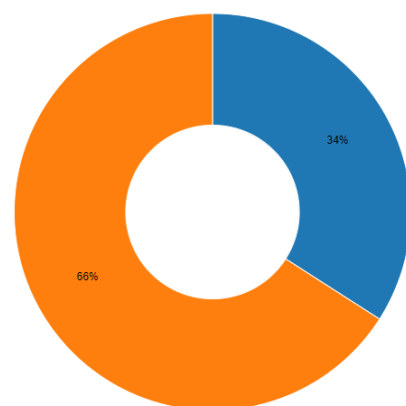


Figure 2: Donut pie chart for Overall total ether received

All the histograms are in two colours: blue and orange. Blue is representing total amount of ether transferred whereas orange is indicating total ether received. The histogram is having two bars on left hand side – embodies ‘fair’ transaction whilst the two bars on the right-hand side embodies ‘fraud’.

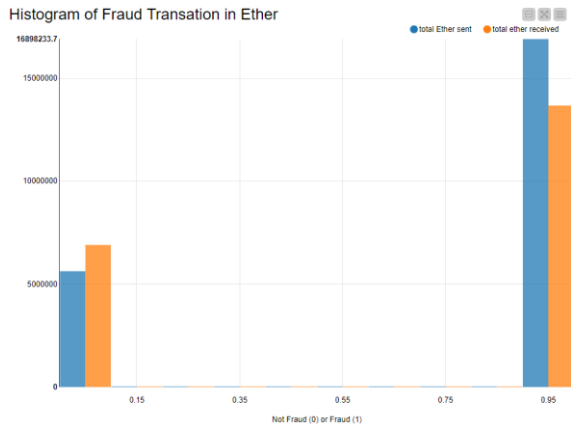


Figure 3: Overall Flag analysis on Ethereum.

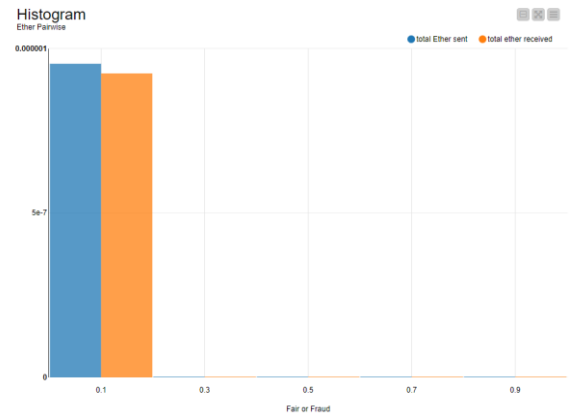


Figure 4: Overall Ethereum Pair-wise Transaction Analysis

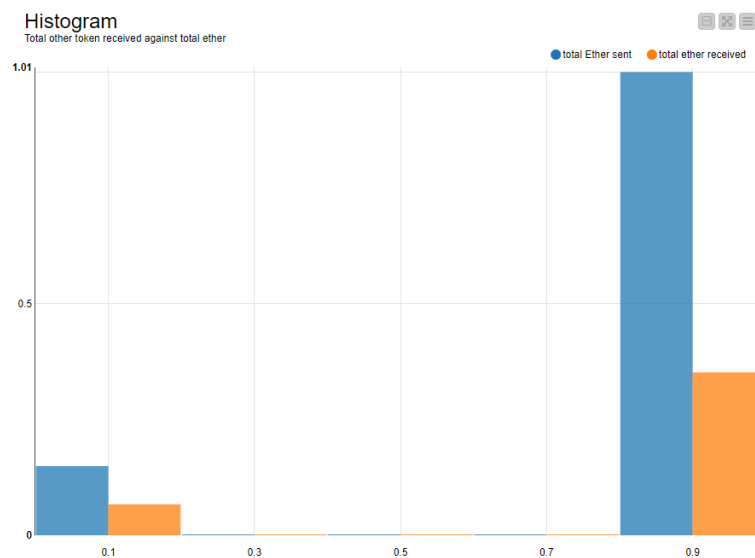


Figure 5: Comparison of Transaction Analysis of Wallet involving transaction between Ethereum and other tokens.

Based on the analysis of Figures 3, 4 and 5, it can be concluded that Ether as a token has been used by wallets that only use Ether as a token for fair purposes. In contrast, if Ether is paired up with other ERC-20 tokens, the addresses have been used for both illicit and legal transactions.

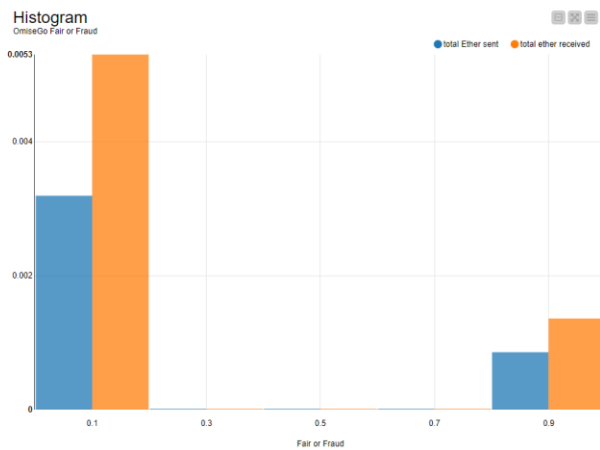


Figure 6: Overall OmiseGo Pair-wise Transaction Analysis

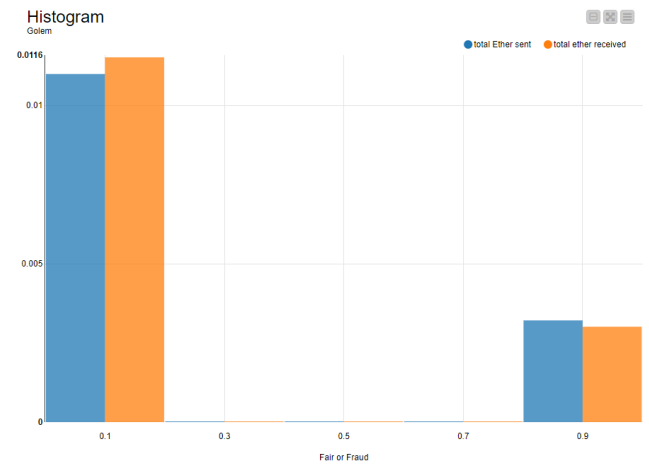


Figure 7: Overall Golem Pair-wise Transaction Analysis

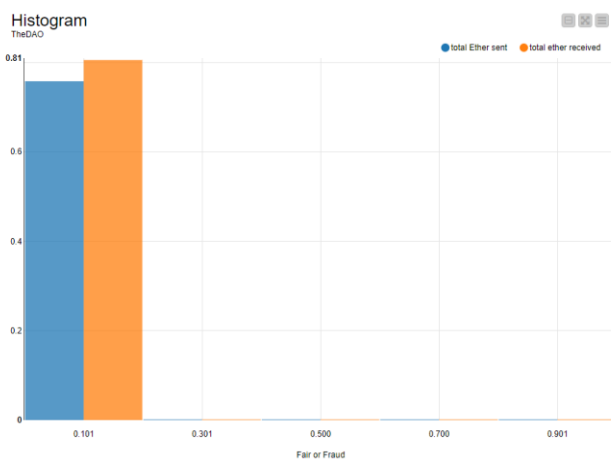


Figure 8: Overall TheDAO Pair-wise Transaction Analysis

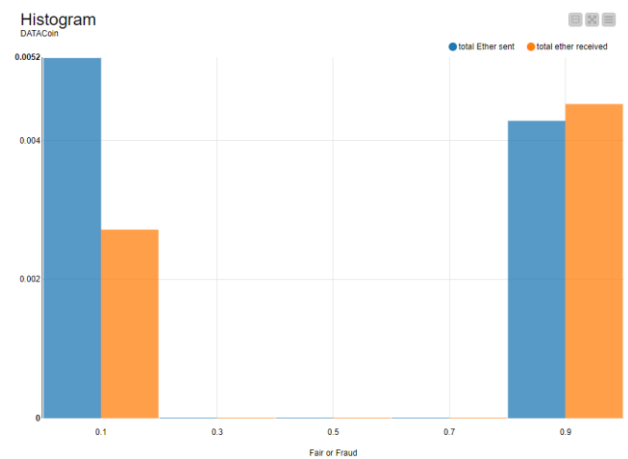


Figure 9: Overall DATACoin Pair-wise Transaction Analysis

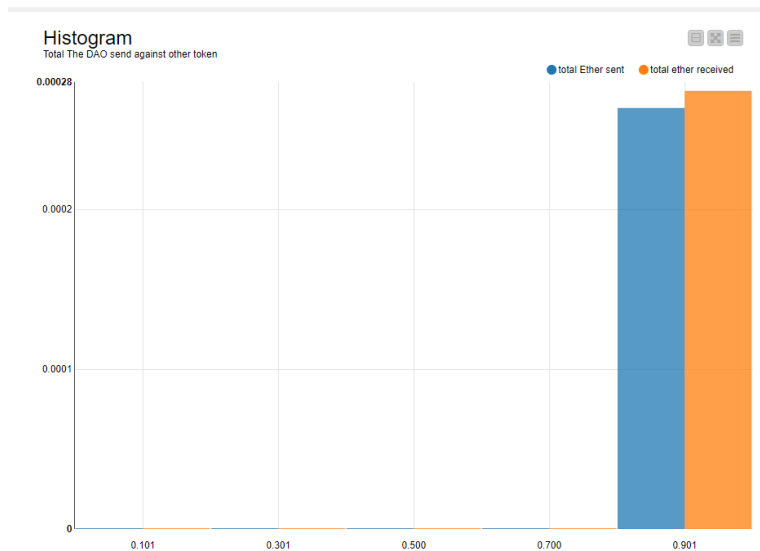


Figure 10: Comparison of Transaction Analysis of Wallet involving transaction between TheDAO and other tokens.

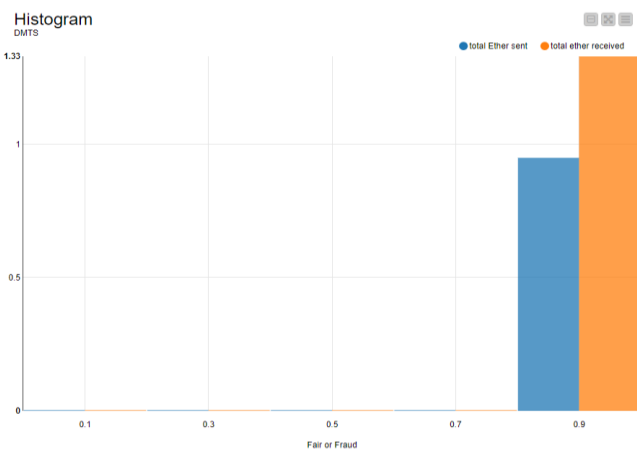


Figure 11: Overall DMTS Pair-wise Transaction Analysis

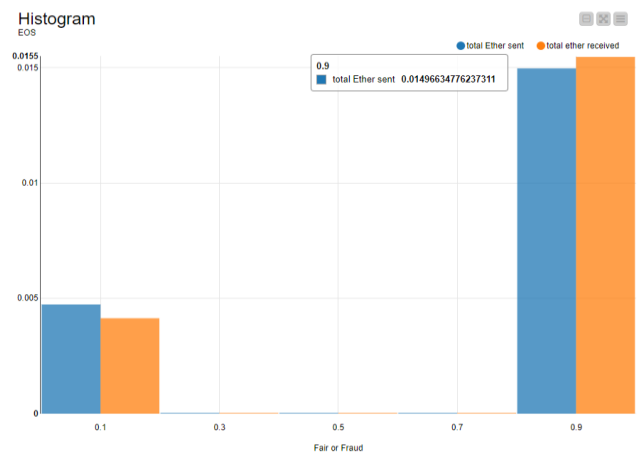


Figure 12: Overall EOS Pair-wise Transaction Analysis

As a result of the analysis of Figures 6 and 7, the tokens OmiseGo and Golem were relatively more frequently used in legal transactions than in illegal transactions. However, tokens such as DATAcoin, DMTS, and EOS are suspicious because they have historically been used in fraud transactions as demonstrated in Figures 9, 11, and 12. In Figure 8, it can be seen that pair-wise transactions between TheDAO were conducted legitimately; nevertheless, if there were transactions between TheDAO and others, every single transaction was flagged as fraudulent.

Four pie charts illustrate a graphical analysis of transaction activity among the eight categorised tokens based on transaction dataset B. The first two charts reflect the transactions conducted by receivers and the latter two illustrate the activities of senders. Figure 14 indicates that DMTS is the second most popular token among receivers (31%). Further, Figure 15 indicates that DMTS also dominates as the second-highest volume of transactions among receivers (21%). In contrast, Ether represents the second most popular token among senders. According to another pie chart, 79% of the total number of transactions involved sending other tokens.

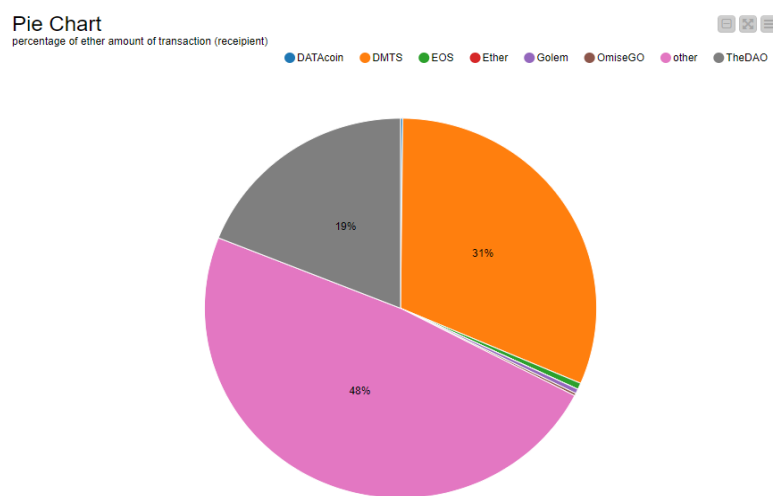


Figure 13

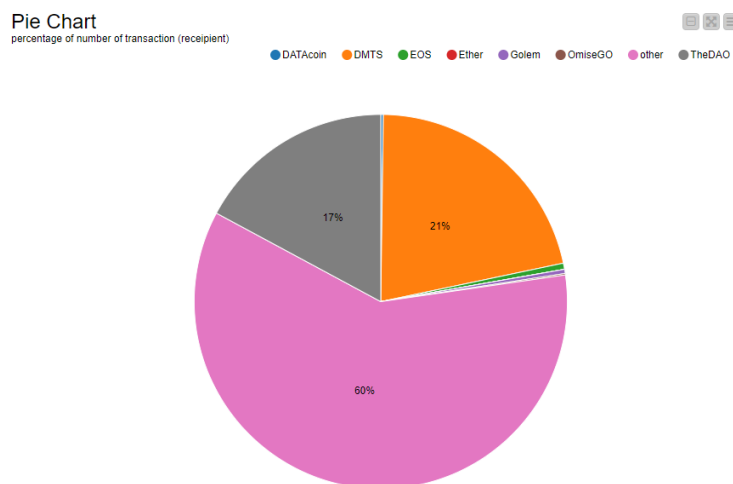


Figure 14

Pie Chart

percentage of number of transaction (sender)

DATAcoin DMTS EOS Ether Golem OmiseGO other TheDAO

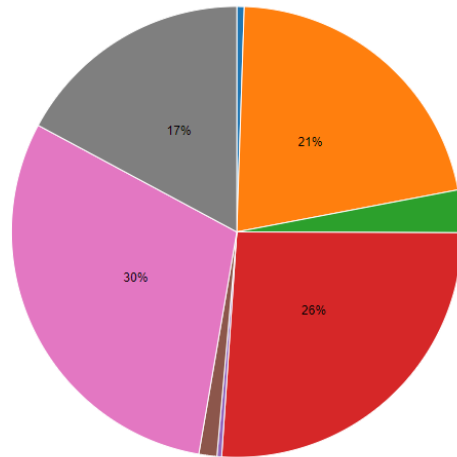


Figure 15

Pie Chart

percentage of ether amount of transaction (sender)

DATAcoin DMTS EOS Ether Golem OmiseGO other TheDAO

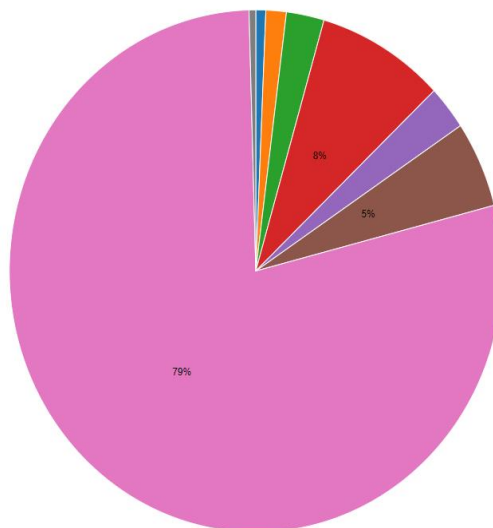


Figure 16

3.4 Data Mining Tasks

Under Data Mining mission, both descriptive and predictive analytical tasks are executed. For descriptive, clustering analysis is done using two different approaches: Principal component analysis (PCA) and t-distributed stochastic neighbor embedding (t-SNE). Whilst, for predictive analysis, regression and classification methodologies are used.

3.4.1 Clustering Analysis

The clustering analysis is executed to identify pattern and outliers among the data (Barnett et al., 1978). It seeks to detect hidden patterns or groupings in a dataset using clustering algorithms. An anomaly detection (also called an outlier detection or novelty detection) refers to identifying rare items, events or observations that differ significantly from the majority of the data and do not conform to a well-defined concept of normal behavior (Lewis, 1978). In this section, two clustering analysis are done - PCA and t-SNE.

PCA is utilized to reduce the dimensionality of large data sets. By transforming a large collection of variables into a smaller collection, a significant amount of information from the large collection is retained. Additionally, PCA allows for easy exploration and visualization of data, as well as highlighting variations and patterns in a dataset as witnessed below in Figure 17.

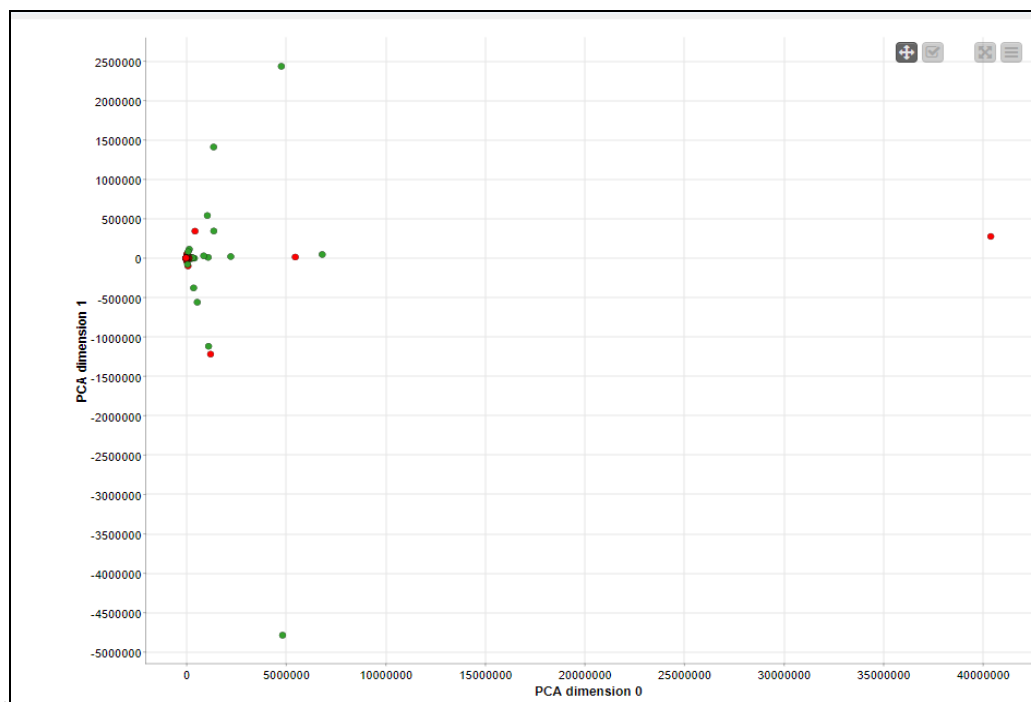


Figure 17 PCA with fair outlier on the negative PCA dimension 1 while fraud outlier on the positive side.

As a method of visualizing high-dimensional data, t-SNE assigns each data point a location on a two- or three-dimensional map. With stochastic neighbor embedding, a probability distribution is constructed for pairs of high-dimensional objects. Figure 18 displays five clusters : four mixture of fraud and fair transactions while one fraud transaction only. Conclusively, there is still a substantial overlap of different class data points present throughout.

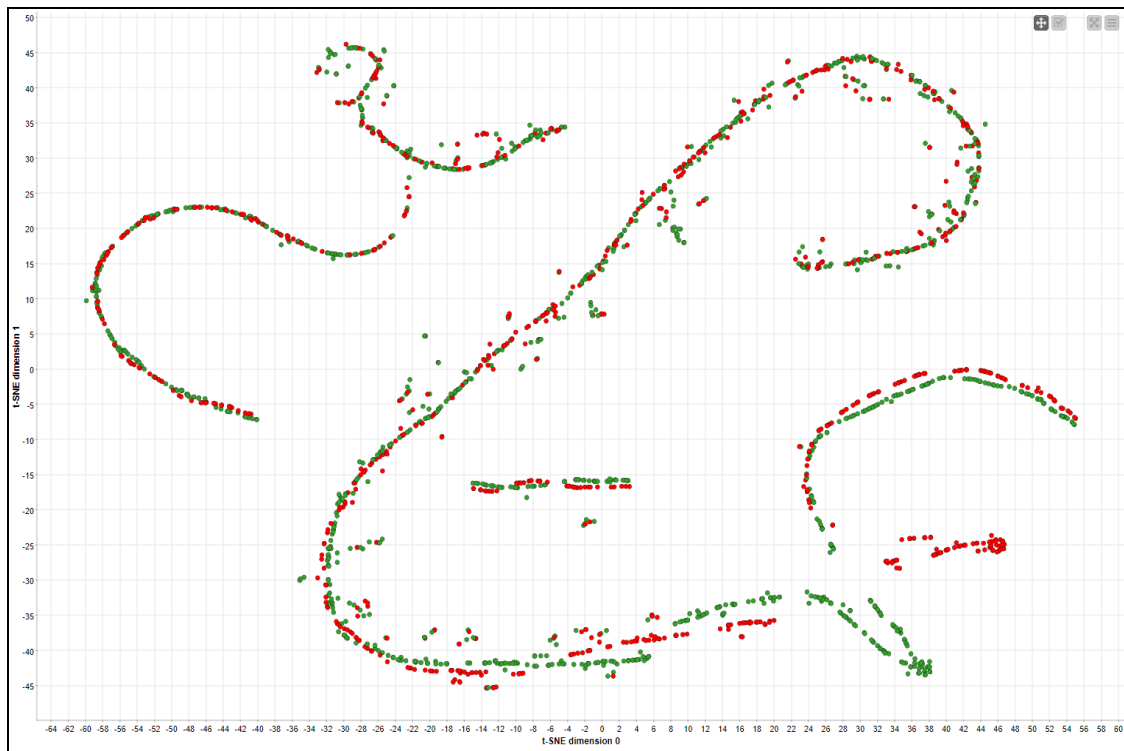


Figure 18 depicts five clusters.

It can be observed that there are arbitrary shaped patterns in PCA and t-SNE. However, as studied by Hillemann et al. (2015), there is the high plausibility of cognitive bias in the form of clustering illusion as such patterns may not exist in real time data. Hence, to further find out the patterns, linear correlation is executed on KNIME.

3.4.2 Linear Correlation

Any statistical relationship between two random variables or bivariate data is referred to as correlation or dependency, and it can reveal a predictive relationship that can be used practically. Correlation does not necessarily indicate cause, though. The linear correlation in Figure 19 reflects that there are the positive relationships among the variables: Sent txn, Received Txn, total Ether sent and total ether received. This implies that their linear

relationship can be formulated among these variables. These will be split into two distinct models: Total Amount of Ether received and Total Amount of Ether transferred.

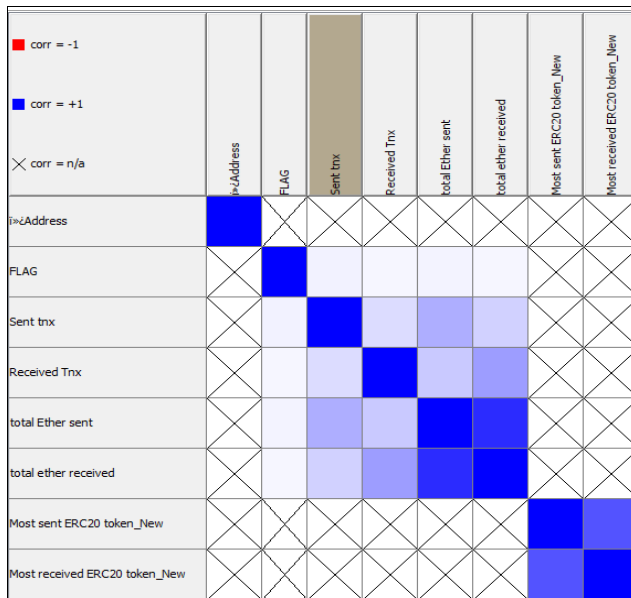


Figure 19 represents the relationship among variables. The darker blue color indicates the stronger is the relationship.

S	First column name	S	Second column name	D	Correlation value	D	p value
FLAG		Sent txn		0.04962412739426...	0.10391885057329864		
FLAG		Received Txn		0.03383426563334...	0.26770753585743323		
FLAG		total Ether sent		0.04628608091111...	0.12935811873575287		
FLAG		total ether received		0.03528893850861...	0.24766512687511466		
Sent txn		Received Txn		0.13709229864685...	6.453601721245761E-6		
Sent txn		total Ether sent		0.31651767803447...	0.0		
Sent txn		total ether received		0.18122944026161...	2.167687140897101E-9		
Received Txn		total Ether sent		0.21137677219752...	2.5297541839108817E-12		
Received Txn		total ether received		0.3834239519334055	0.0		
total Ether sent		total ether received		0.8309637856328667	0.0		
Most sent ERC20 token_ New		Most received ERC20 token_ New		0.6750467709984359	0.0		

Figure 20 is the table extracted from KNIME.

This table in Figure 20 outlines that the relationships between the following variables are positive, moderate and statistically significant (because p-value is less than 0.05):

- Sent txn and Received Txn
- Sent txn and total Ether sent
- Sent Txn and total ether received
- Received Txn and Total Ether sent
- Received Txn and total ether received
- total Ether sent and total ether received

- Most sent ERC20 token_New and Most received ERC20 token_New

Below two diagrams (Figure 21 and Figure 22) are dispersion analysis in the form of the box plots extracted from KNIME for the variables containing continuous numeric data.

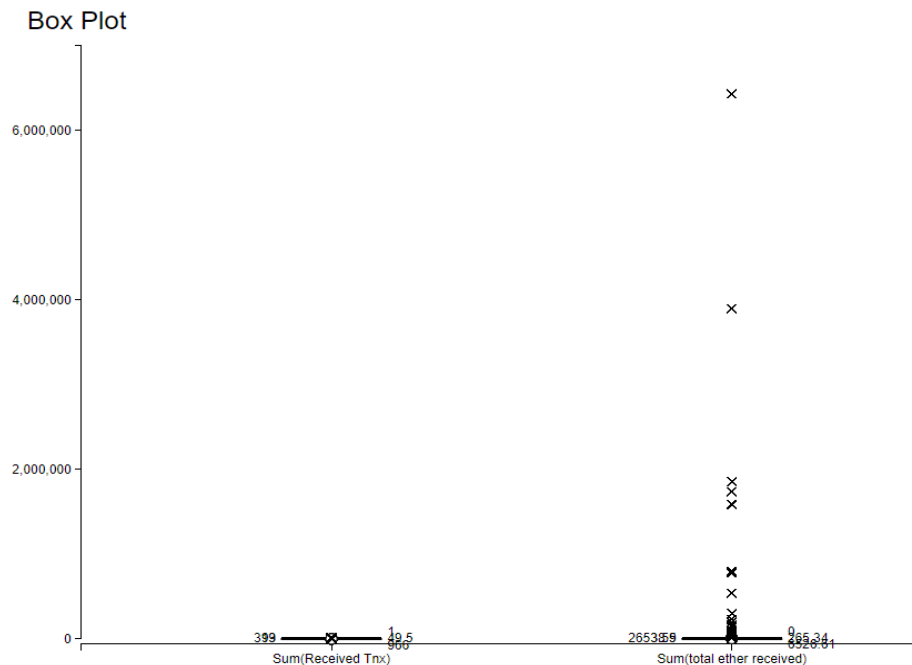


Figure 21 shows that the boxplots for both variables- 'Received Tnx' and 'total ether received'. In the data of variable, total ether received, there are significant number of outliers.

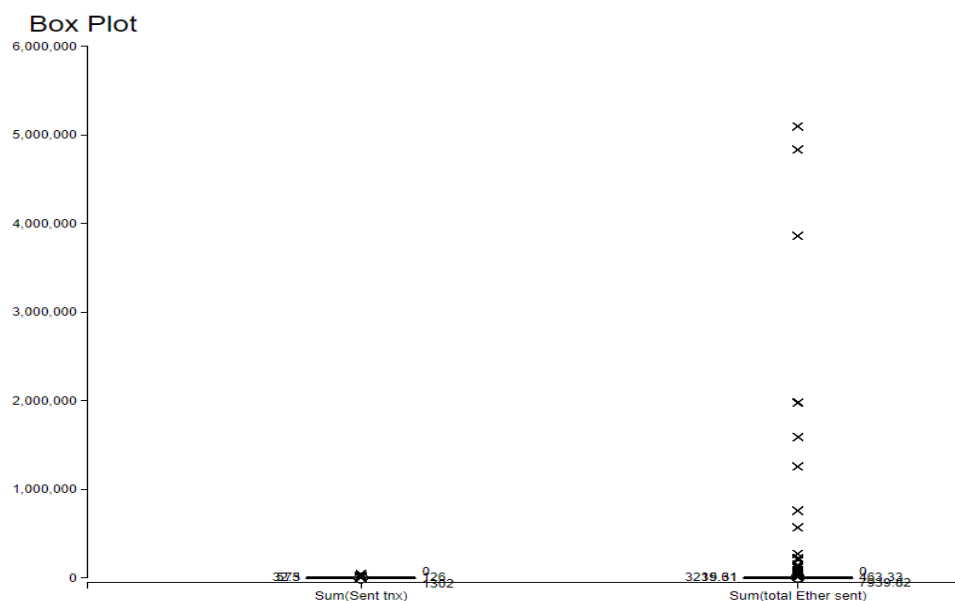


Figure 22 shows that the boxplots for both variables - 'Sent Tnx' and 'total ether sent'. In the data of variable, total ether sent, there are significant number of outliers.

The results of numerous data description studies indicate that the Ethereum dataset may be used to develop predictive models. However, in light of the fact that there are outliers, the models formulated should be tested for their fitness. The next section will provide an overview of ten models, along with a fitness test for each of them.

3.4.2 Multiple Linear Regression Modelling

For predictive analytical tasks, linear regression and classification methodologies are applied to project the future events after training the past data. To generate the multiple linear regression among variables, the heteroscedasticity of the residuals, and the normality of the residuals, KNIME (Appendix A, figure 8) is used. The following Table 2 represents the variables assigned to the Field of Interest defined as in table 1.

Field of Interest	Variable
FLAG	F
Sent tnx	A
Received Tnx	B
total ether received	C
total Ether sent	D

Table 2: Variable Name for Field of Interest

Multilinear Regression Model for ‘Total Amount of Ether Transferred’ = D :

The new simple fit model for D is as follows:

$$D = 0.001F + 0.093A - 0.057B + 0.963C - 0.001$$

Although Figure 23 depicts there is a residual have weak heteroskedastic, D model’s R-squared value is 0.7 and normal distribution of standard error (Figure 22) further justify that the following equation can be run to predict the total amount of ether transferred. So, as per D’s equation , for every flagged transaction, there is an average increase of 0.001 ether in the average total amount of total ether transferred. Likewise, for every one unit of token transfer, there is an average increase of 0.0093 ether in the total amount of ether transferred. Similarly, for every one unit of ether received, there is an average 0.963 ether increase in the average amount of total ether transferred. However, for every one unit of token received, there is an average of 0.057 ether decrease in total amount of ether transferred.

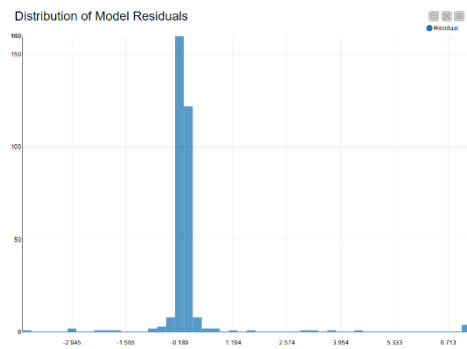


Figure 23: Normally Distributed Histogram of standard errors

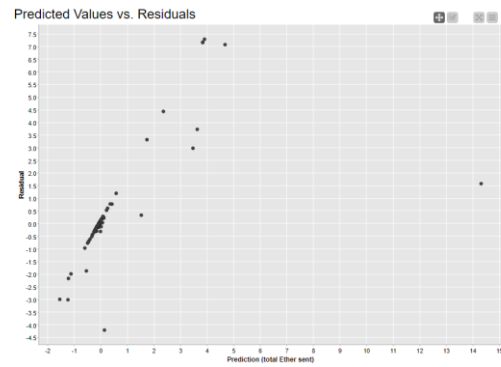


Figure 24: Residuals' heteroskedasticity test

Multilinear Regression Model for 'Total Amount of Ether Received' = C :

The new simple linear model for C is as follows:

$$C = -0.037A + 0.048B + 0.738D$$

Visually, Figure 26 indicates the presence of heteroskedasticity and Figure 25 implies that the residuals are not normally distributed. Together with negative R-squared value of -0.632, random scatterplot and not achieving normal distribution for the residual, the model for C is mis specified and misfit for future usage.

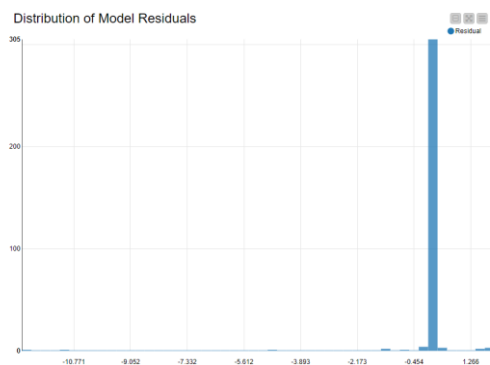


Figure 25: Not Normally Distributed Histogram of standard errors

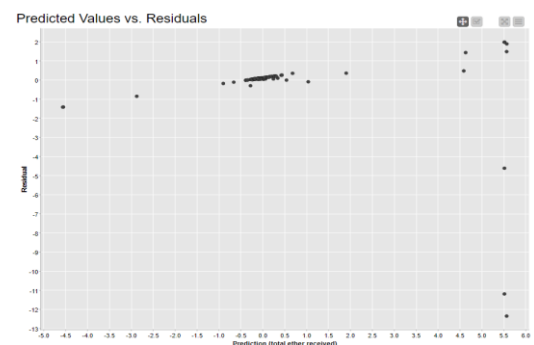


Figure 26: Not Normally Distributed Histogram of standard errors

3.4.3 Classification Analysis

This study uses KNIME to generate eight classification models (see Appendix A, Figures 9, 10, 11 and 12 for additional information). A decision tree classifier, a random forest classifier, a gradient booster model, and an extreme gradient booster model are separately developed using two datasets A and B. To ensure that both fraud and fair transactions are represented in the training and test sets, stratified sampling is employed, ensuring that both

classes are proportionately represented in the final subset, based on the original distribution of classes. This analysis utilizes the SMOTE algorithm presented by Chawla et al. (2002) in order to produce a better classification model. By adjusting the distribution of classes, it improves supervised learning algorithms' classification performance. In Cohen (1988), Kappa results are interpreted as follows: 0 indicates no agreement, 0.01-0.20 indicates little or no agreement, 0.21-0.40 indicates fair agreement, 0.41- 0.60 indicate moderate agreement, 0.61- 0.80 indicates substantial agreement, and 0.81-1.00 indicates almost perfect agreement. In addition to the area under curve (AUC), receiver operating characteristic curves (ROC curves) provide additional indicators of model fitness (Bruce et al., 2017).

3.4.3.1 Decision Tree Modelling

It is a non-parametric supervised learning method used for classification and regression. It aims to create a model that predicts the value of a target variable by learning simple decision rules inferred from the data features. Table 3 represents the confusion matrices for decision tree classifier outcomes based on both dataset A and B. Based on Cohen's criteria, with dataset A, the model is moderate for classification whereas with dataset B, the model is evaluated at fair level.

Table 3: Confusion Matrices for Decision Tree Models

Decision Tree model Confusion Matrix (dataset A)		
	Fair (Predicted)	Fraud (Predicted)
Fair (Actual)	240	106
Fraud (Actual)	74	225
Correctly classified: 465		Wrongly classified: 180
Accuracy: 72.09%		Error: 27.91%
Cohen's kappa (K): 0.443%		
Decision Tree model Confusion Matrix (dataset B)		
	Fair (Predicted)	Fraud (Predicted)
Fair (Actual)	256	90
Fraud (Actual)	104	195
Correctly classified : 451		Wrongly classified: 194
Accuracy: 71.11%		Error: 30.08%
Cohen's kappa (K): 0.393%		

3.4.3.2 Random Forest Modelling

Random forest is a technique used in behaviour predictions and behaviour analysis and is built on decision trees. It contains many decision trees that represent a distinct instance of the classification of data input into the random forest. Each individual tree in the random forest spits out a class prediction and the class with the most votes becomes model's prediction.

Table 4 presents the confusion matrices for Random Forest classifier outcomes for datasets A and B. According to Cohen's criteria, with both datasets, the model is sufficiently robust to be deployed in the future, since their kappa value is between 0.61% and 0.80%.

Table 4: Confusion Matrices for Random Forest Models

Random Forest Modelling Confusion Matrix (Dataset A)		
	Fair (Predicted)	Fraud (Predicted)
Fair (Actual)	309	37
Fraud (Actual)	31	268
Correctly classified: 577		Wrongly classified: 68
Accuracy: 89.46%		Error: 10.54%
Cohen's kappa (K): 0.788 %		
Random Forest Modelling Confusion Matrix (Dataset B)		
	Fair (Predicted)	Fraud (Predicted)
Fair (Actual)	310	36
Fraud (Actual)	44	255
Correctly classified : 565		Wrongly classified: 80
Accuracy: 87.6%		Error: 12.4%
Cohen's kappa (K): 0.750%		

3.4.3.3 Gradient Boost Modelling

Gradient boosting is a machine learning technique used in regression analysis and classification. The model provides a prediction in the form of an ensemble of weak prediction models, typically decision trees. When a decision tree is the weak learner, a gradient-boosted tree is produced and usually outperforms a random forest algorithm (Piryonesi, et al., 2020). As measured by Cohen's criteria, the Gradient Boosting Model has moderate effectiveness, as its kappa value ranges from 0.41% to 0.60% as displayed in table 5.

Table 5: Confusion Matrices for Gradient Boosting Models

Confusion Matrix: Gradient Boosting Modelling (Dataset A)		
	Fair (Predicted)	Fraud (Predicted)
Fair (Actual)	280	66
Fraud (Actual)	81	218
Correctly classified : 496		Wrongly classified: 147
Accuracy: 77.21 %		Error: 22.79 %
Cohen's kappa (K): 0.540%		
Confusion Matrix: Gradient Boosting Regression (Dataset B)		
	Fair (Predicted)	Fraud (Predicted)
Fair (Actual)	284	62
Fraud (Actual)	101	198
Correctly classified :482		Wrongly classified: 163
Accuracy: 74.73 %		Error: 25.27 %
Cohen's kappa (K): 0.487%		

3.4.3.4 Extreme Gradient Boost Modelling

Kaggle's machine learning competition in 2015 featured over half of the winning solutions that used XGBoost (Zhang et al., 2018). The most commonly used method for identifying patterns of anomalous behavior is Extreme Gradient Boosting (XGBoost). The XGBoost algorithm is a decision tree ensemble Machine Learning algorithm that utilizes a gradient boosting architecture. In contrast to gradient boosting machines based on the same architecture, it is 20 times faster and can scale to billions of instances while requiring sparse resources. In this model, three main importance metrics are provided to quantify the

importance of all features, namely weight, gain and cover. It is a matrix with the first column listing the features and the other columns defining the importance value in relation to the importance metric. In accordance with Cohen's criteria, the Extreme Gradient Boosting Model is substantially significant, as its kappa value ranges from 0.61% to 0.80% (table 6).

Table 6: Confusion Matrices for Extreme Gradient Boosting Models

XGBoost Modelling (Dataset A)		
	Fair (Predicted)	Fraud (Predicted)
Fair (Actual)	284	52
Fraud (Actual)	43	256
Correctly classified : 550		Wrongly classified: 95
Accuracy: 85.27 %		Error: 14.73 %
Cohen's kappa (K): 0.704 %		
Table 2: XGBoost Modelling (Dataset B)		
	Fair (Predicted)	Fraud
Fair (Actual)	305	41
Fraud (Actual)	51	248
Correctly classified: 553		Wrongly classified: 92
Accuracy: 85.74%		Error: 14.26%
Cohen's kappa (K): 0.713 %		

3.4.3.5 Classification Model Results

After assessing the eight classification models along with their results in the previous section, this section will justify its selection of Random Forest Classifier for the detection of fraudulent activities on Ethereum Blockchain. As an indicator of model fitness, ROC and AUC are commonly used (Bruce et al., 2017). These two criteria were used to formulate the ranking algorithm, as demonstrated in Figures 9 and 10 of Appendix A. This analysis has led to the selection of the Random Forest Model as the best-fit model for dataset A (see Figure 26 and Figure 27) having Cohen's Kappa(%) of 0.788, an average accuracy of 0.8946, and an average AUC of 0.939; and dataset B (see Figure 28 and Figure 29) having Cohen's Kappa(%) of 0.750, an average accuracy of 0.876 and an average AUC of 0.949, respectively. Conversely, the least fit classifier is Decision Tree with dataset A (see Figure

27 and Figure 28) having Cohen's kappa(%) of 0.443 and an average accuracy of 0.72 as well as an average AUC of 0.767, and dataset B (see Figure 29 and Figure 30) having Cohen's kappa(%) of 0.393, an average accuracy of 0.6992 and an average AUC of 0.785, respectively.

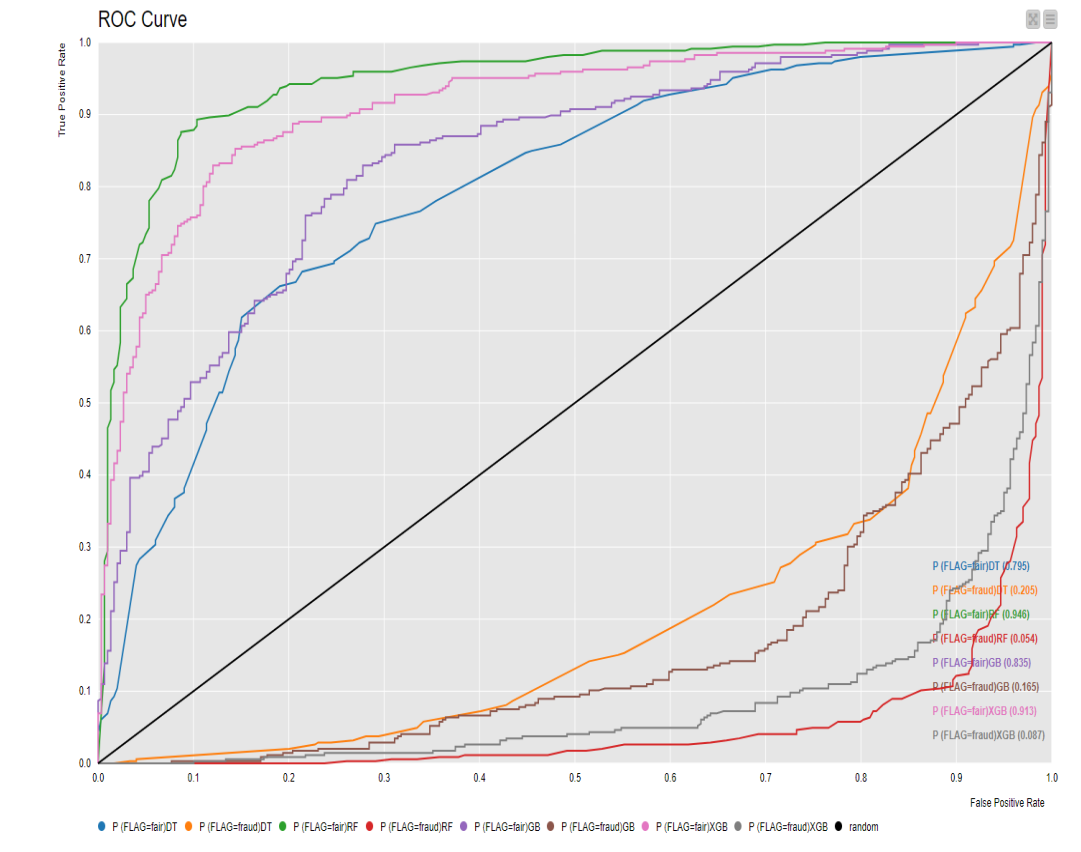


Figure 27: ROC for four classified models based on dataset A

Row ID	Area Under Curve
P (FLAG=fair)DT	0.767
P (FLAG=fraud)DT	0.233
P (FLAG=fair)RF	0.939
P (FLAG=fraud)RF	0.061
P (FLAG=fair)GB	0.808
P (FLAG=fraud)GB	0.192
P (FLAG=fair)XGB	0.913
P (FLAG=fraud)XGB	0.087

Figure 28: Area Under Curve value for models with dataset A.

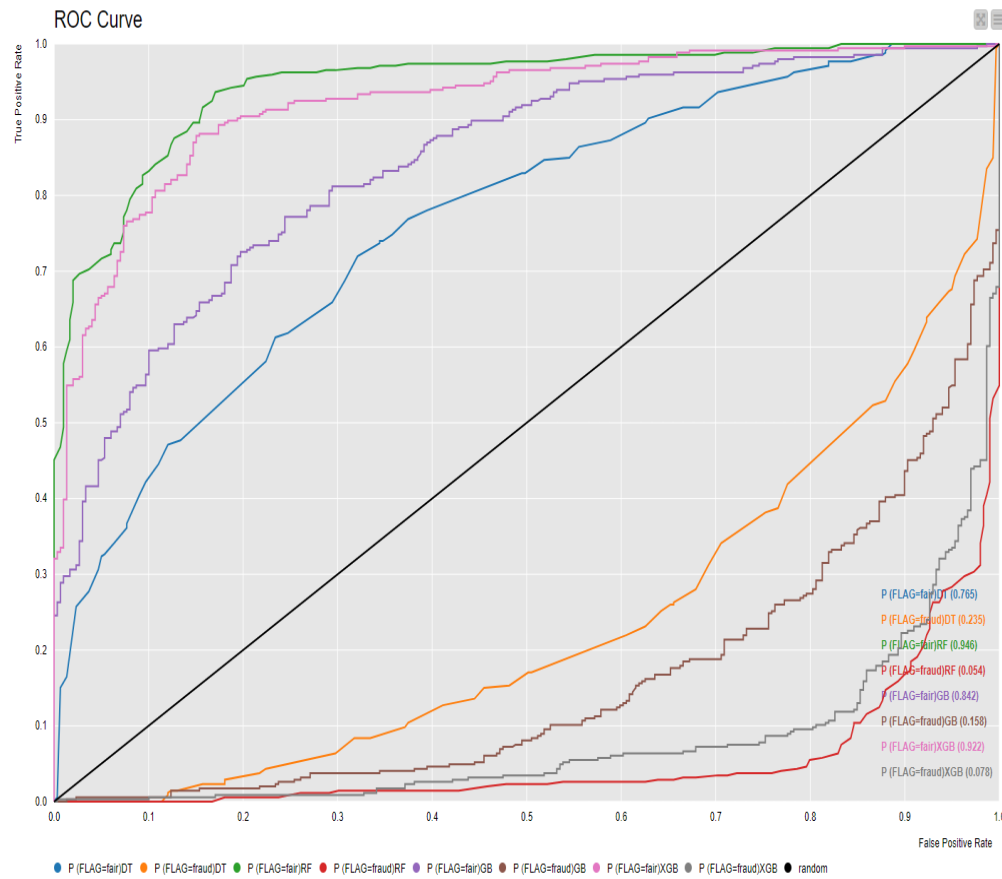


Figure 29: ROC for four classification models based on dataset B.

Row ID	Area Under Curve
P (FLAG=fair)DT	0.785
P (FLAG=fraud)DT	0.215
P (FLAG=fair)RF	0.949
P (FLAG=fraud)RF	0.051
P (FLAG=fair)GB	0.856
P (FLAG=fraud)GB	0.144
P (FLAG=fair)XGB	0.931
P (FLAG=fraud)XGB	0.069

Figure 30: Area Under Curve value for models with dataset B.

4. Conclusion

Considering the results of the data mining, it is evident that the Random Forest Classification method is an extremely effective means of detecting illegitimate Ethereum accounts. Despite this, there are internal validity issues with the models since the SMOTE and normalizer nodes were used during the execution process. Without these nodes, the classification models' performances are substandard. Moreover, the box plots and clustering analysis were found to contain outliers. In addition, after reviewing the descriptive histogram of EOS and Ether and cross-checking them with news (Reynolds, 2022), it appears that the charts are misleading and indicate sampling bias. To predict the future, it will therefore be premature to finalize the implementation of the Random Forest Model and the multiple linear regression model (D's equation). Therefore, neither model can be generalized. For this study to be externally valid and reliable, higher quality and larger volumes of data must be trained (Bruce et al., 2017). Further research and data should be collected to validate the results. Moreover, other techniques should be examined in order to be applied in a real-life situation.

5. Appendix A – Workflow Diagram

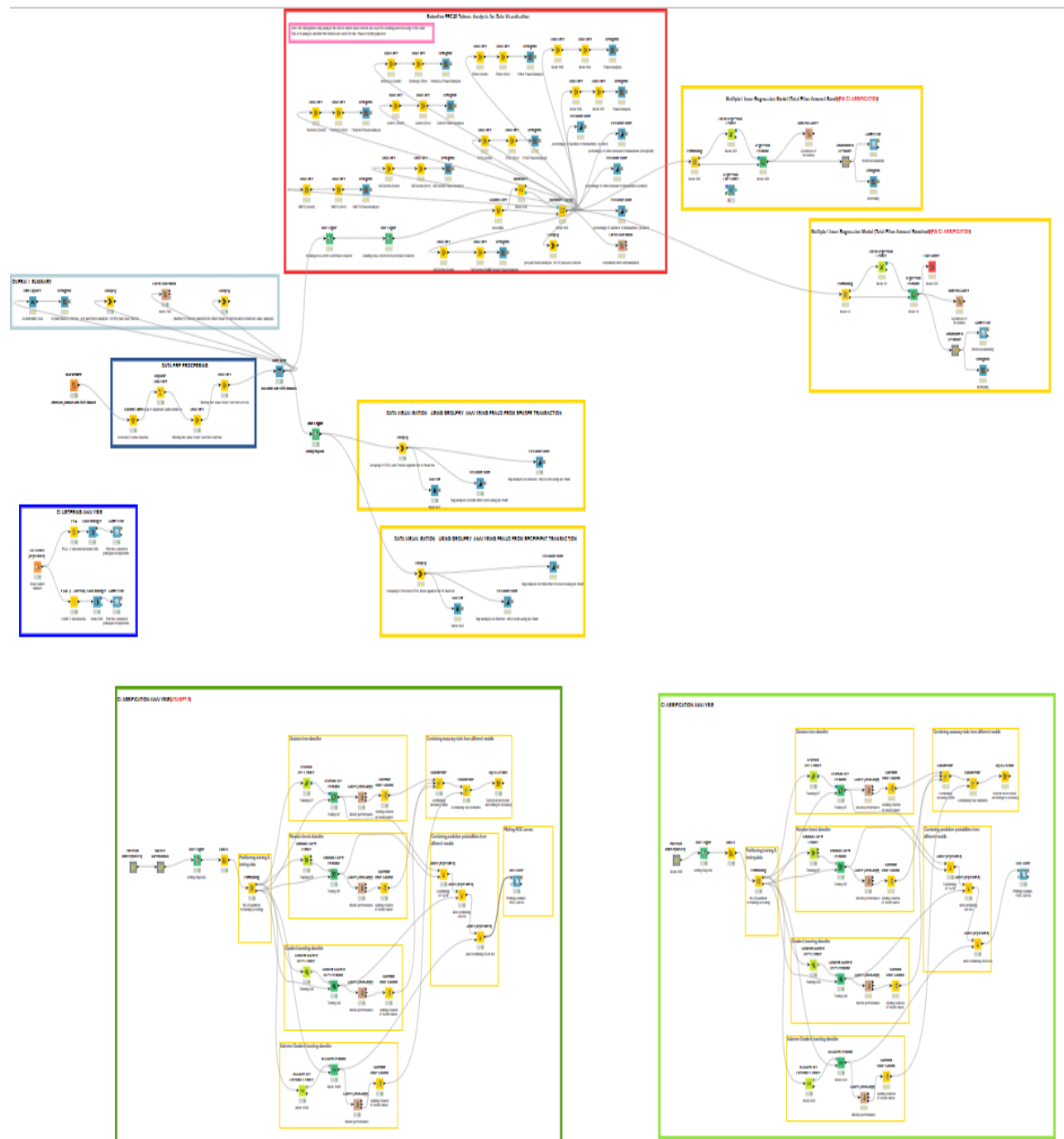


Figure 1: Overview of the workflow

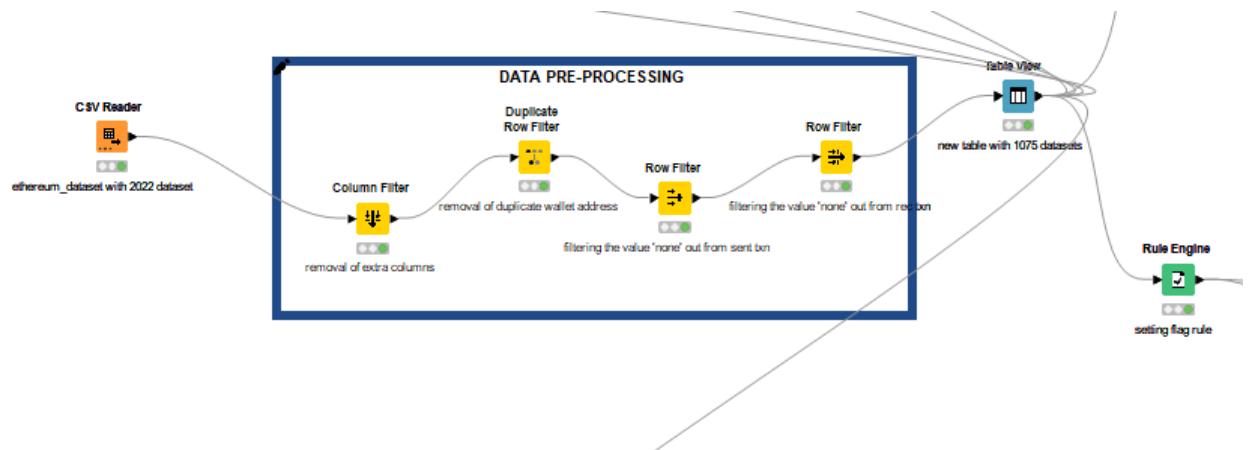


Figure 2 : Data Pre-Processing Task

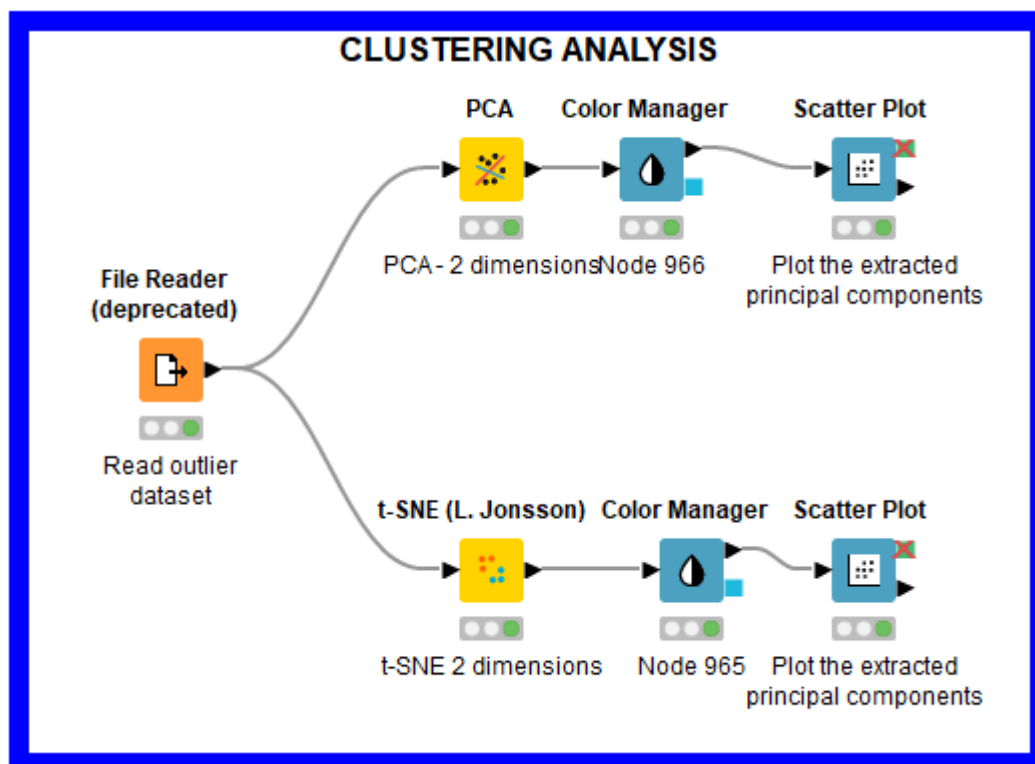


Figure 3: Clustering Analysis

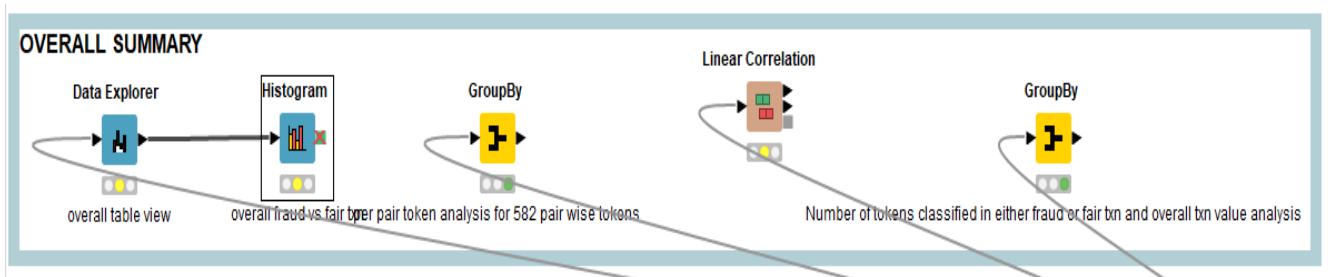


Figure 4: Overall Data Description

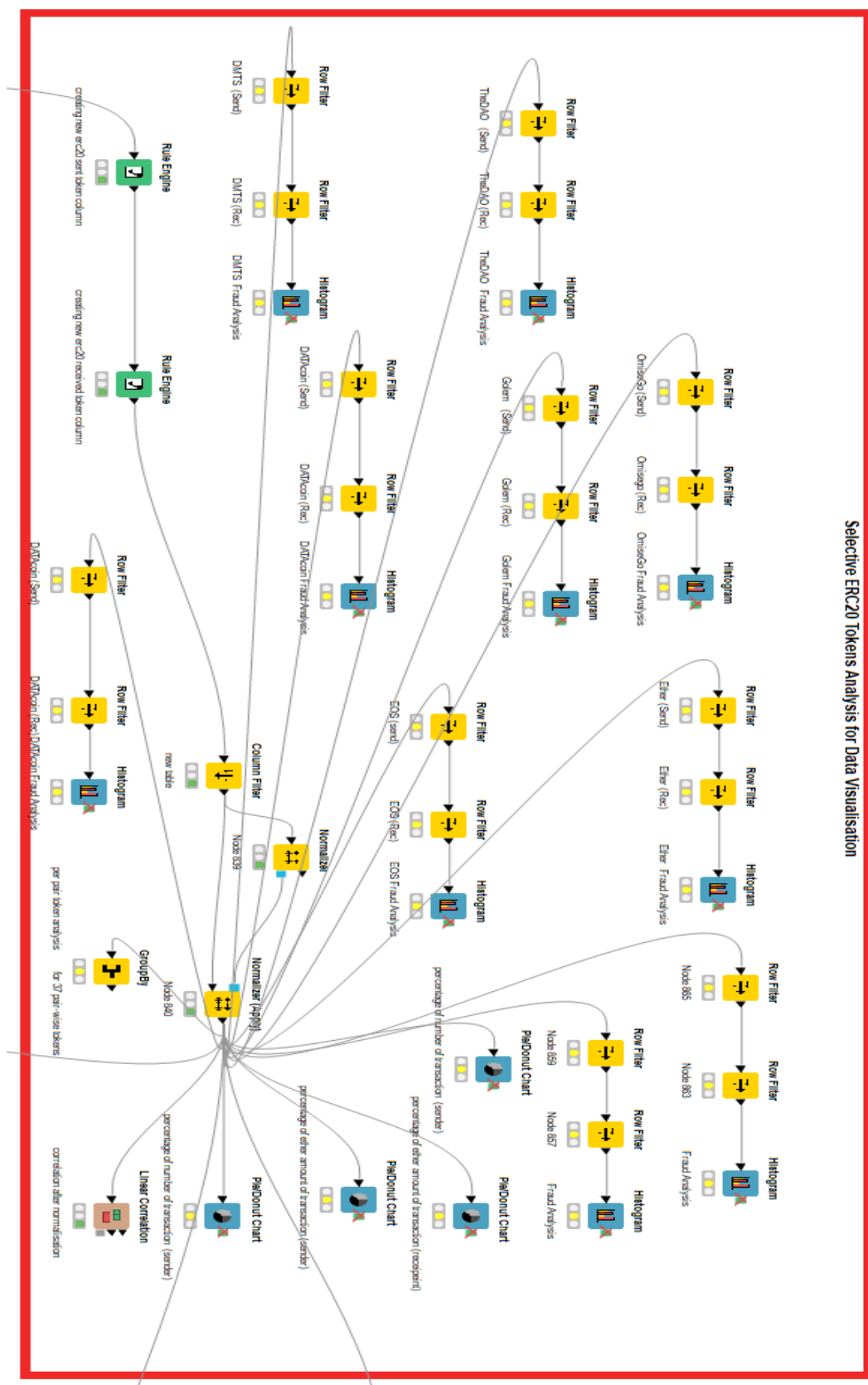


Figure 2: Data Visualisation for selective tokens

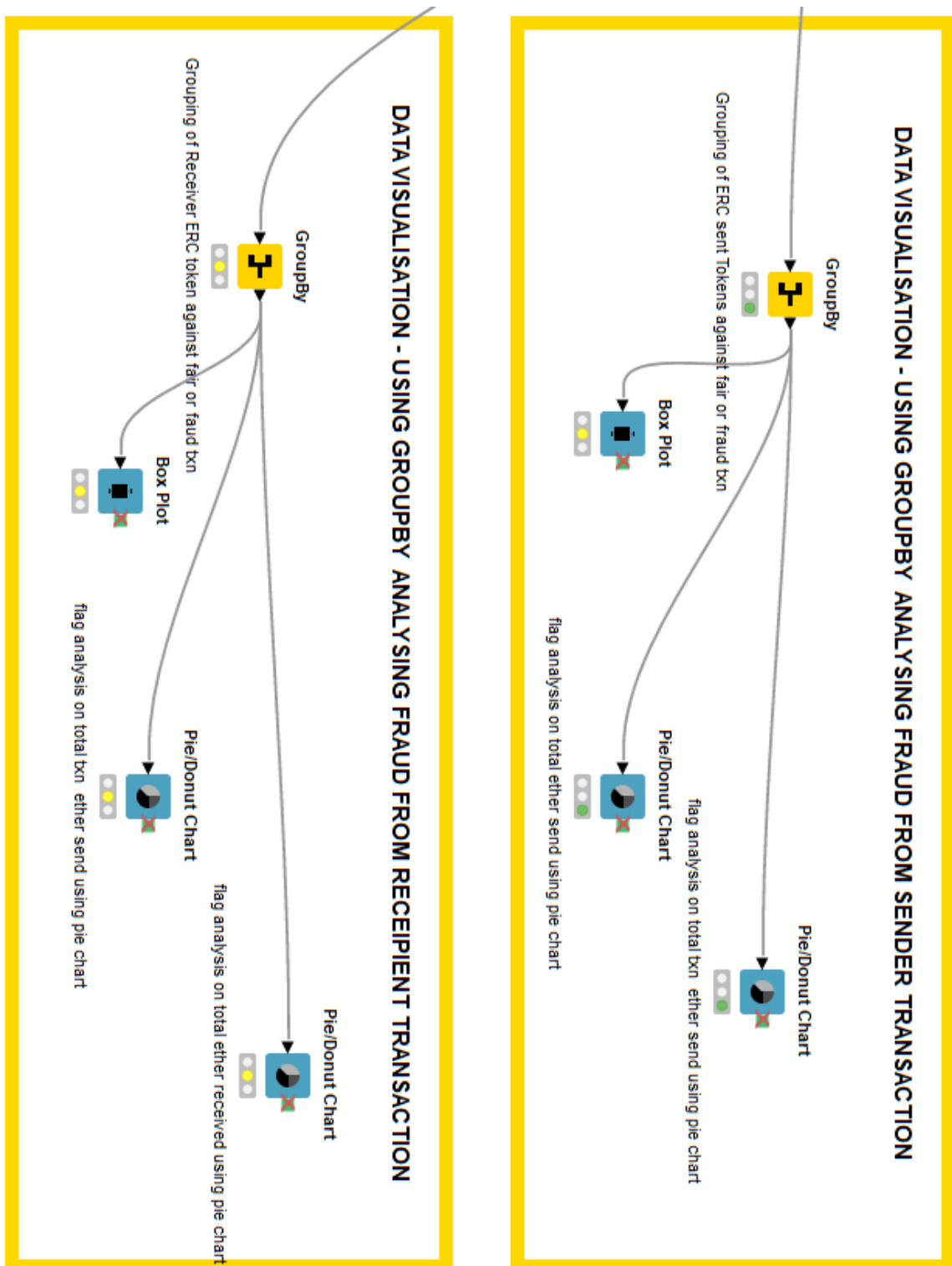


Figure 3: Data visualisation for numeric data

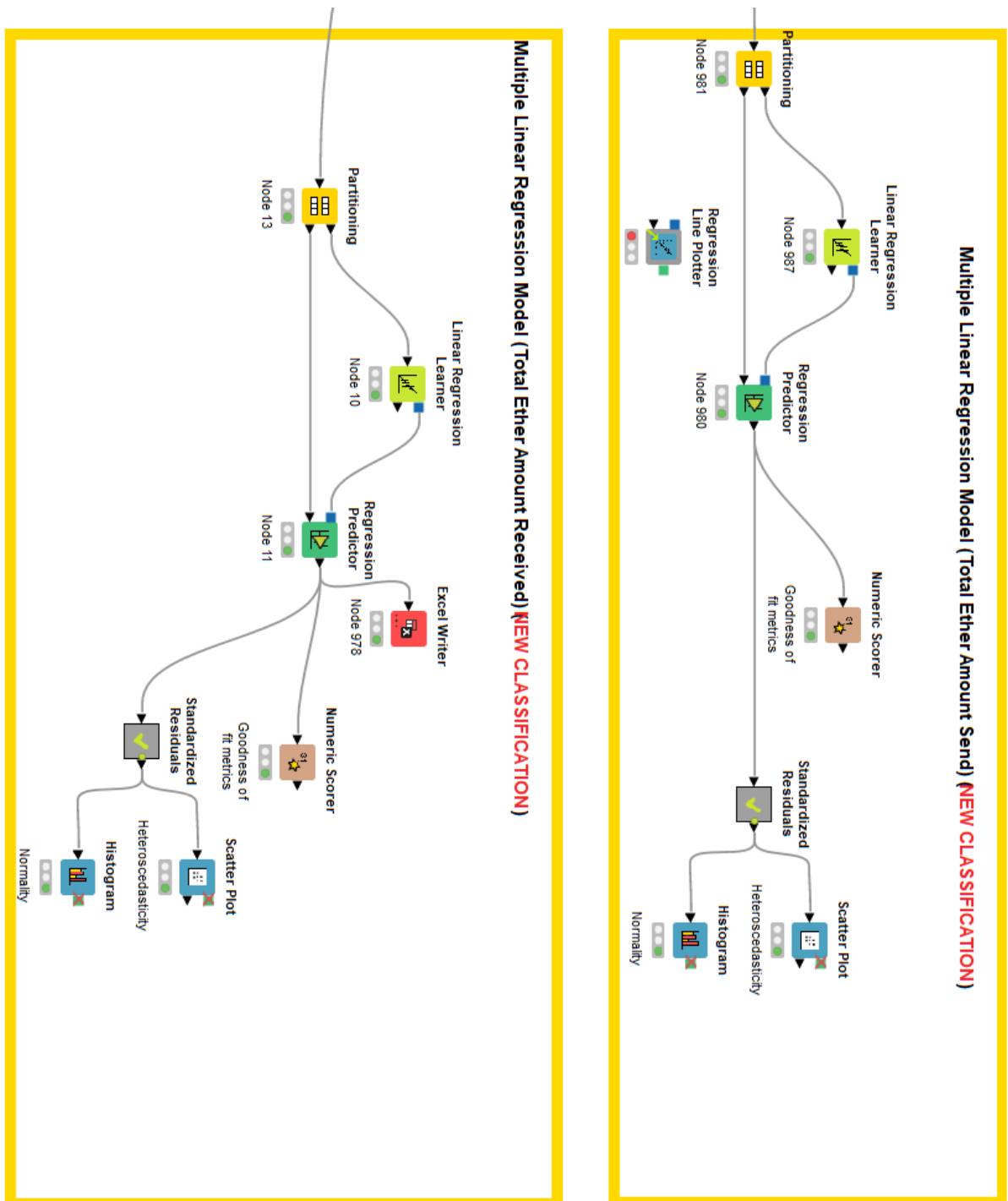


Figure 4 : Multiple Linear Regression Models based on newly categorised tokens.

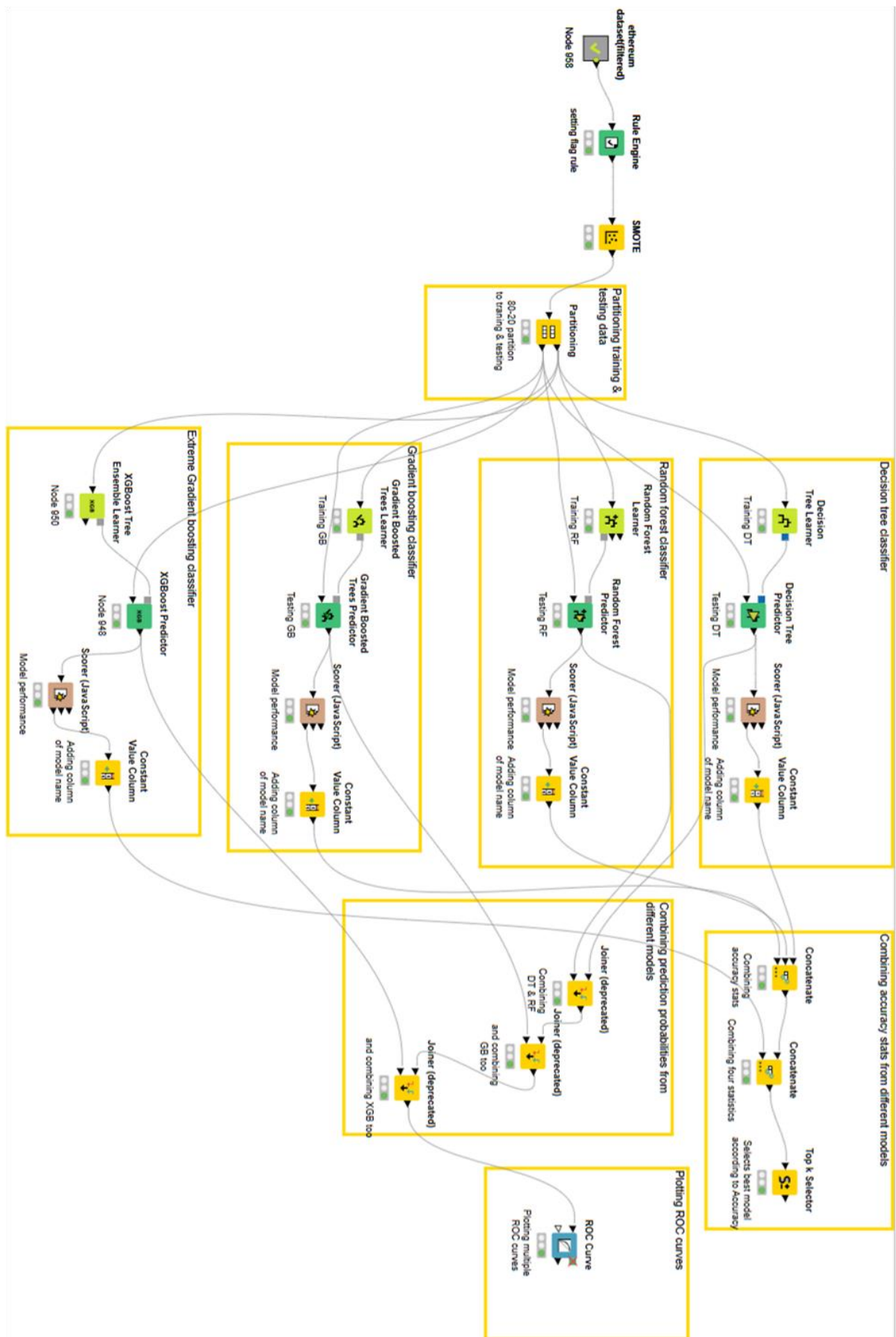


Figure 5: Classification Models based on dataset A.

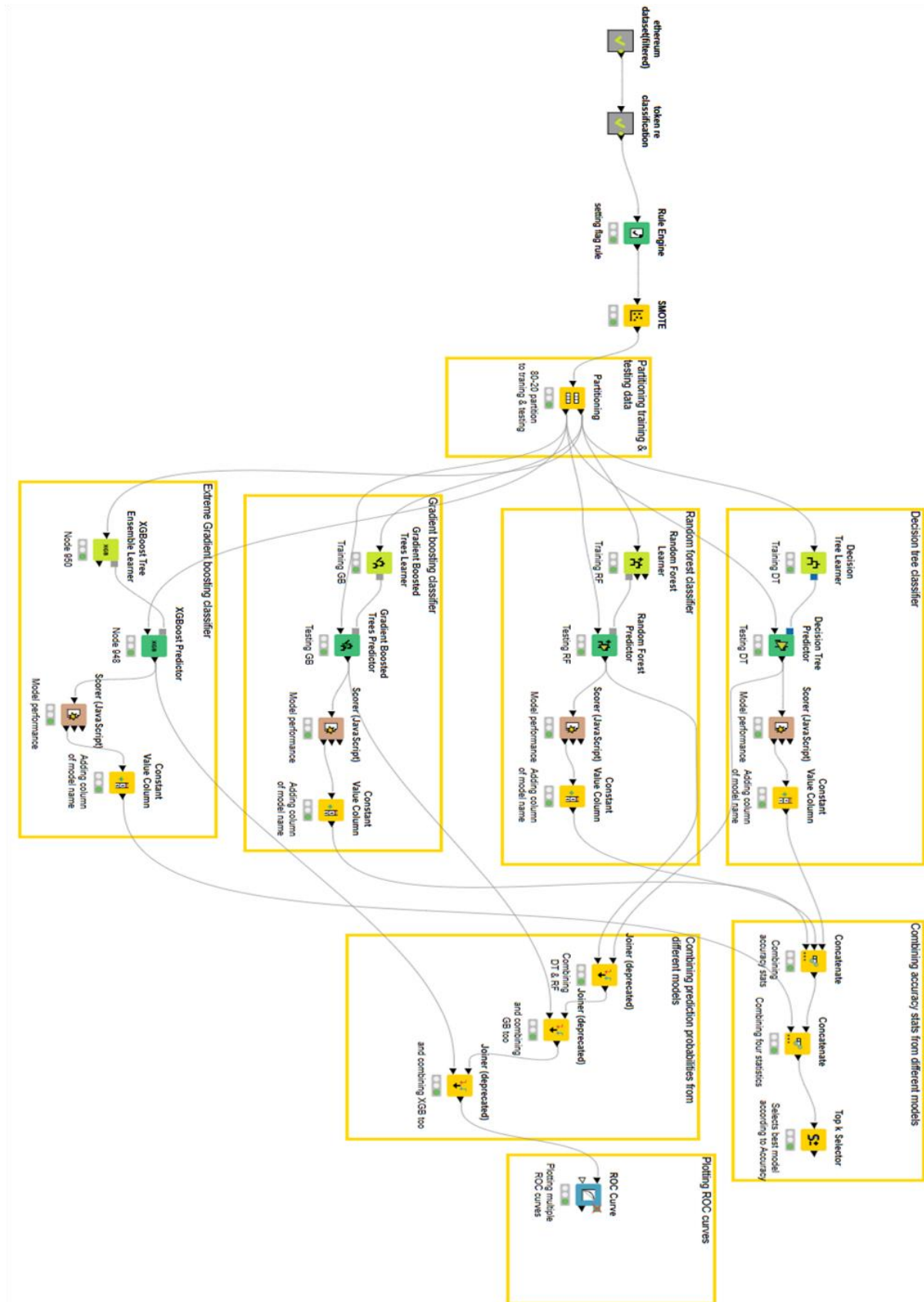


Figure 6: Classification Models based on dataset with dataset B

Decision Tree

Confusion Matrix

	fair (Predicted)	fraud (Predicted)	
fair (Actual)	240	106	69.36%
fraud (Actual)	74	225	75.25%
	76.43%	67.98%	

Overall Statistics

Overall Accuracy	Overall Error	Cohen's kappa (κ)	Correctly Classified	Incorrectly Classified
72.09%	27.91%	0.443	465	180

Random Forest

Confusion Matrix

	fair (Predicted)	fraud (Predicted)	
fair (Actual)	309	37	89.31%
fraud (Actual)	31	268	89.63%
	90.88%	87.87%	

Overall Statistics

Overall Accuracy	Overall Error	Cohen's kappa (κ)	Correctly Classified	Incorrectly Classified
89.46%	10.54%	0.788	577	68

Gradient Boost

Confusion Matrix

	fair (Predicted)	fraud (Predicted)	
fair (Actual)	280	66	80.92%
fraud (Actual)	81	218	72.91%
	77.56%	76.76%	

Overall Statistics

Overall Accuracy	Overall Error	Cohen's kappa (κ)	Correctly Classified	Incorrectly Classified
77.21%	22.79%	0.540	498	147

Extreme Gradient Boost

Confusion Matrix

	fair (Predicted)	fraud (Predicted)	
fair (Actual)	294	52	84.97%
fraud (Actual)	43	256	85.62%
	87.24%	83.12%	

Overall Statistics

Overall Accuracy	Overall Error	Cohen's kappa (κ)	Correctly Classified	Incorrectly Classified
85.27%	14.73%	0.704	550	95

Figure 7: KNIME's output of Confusion Matrices of four distinct classification models based on dataset A.

Decision Tree

Confusion Matrix

	fair (Predicted)	fraud (Predicted)	
fair (Actual)	256	90	73.99%
fraud (Actual)	104	195	65.22%
	71.11%	68.42%	

Overall Statistics

Overall Accuracy	Overall Error	Cohen's kappa (κ)	Correctly Classified	Incorrectly Classified
69.92%	30.08%	0.393	451	194

Random Forest

Confusion Matrix

	fair (Predicted)	fraud (Predicted)	
fair (Actual)	310	36	89.60%
fraud (Actual)	44	255	85.28%
	87.57%	87.63%	

Overall Statistics

Overall Accuracy	Overall Error	Cohen's kappa (κ)	Correctly Classified	Incorrectly Classified
87.60%	12.40%	0.750	565	80

Gradient Boost

Confusion Matrix

	fair (Predicted)	fraud (Predicted)	
fair (Actual)	284	62	82.08%
fraud (Actual)	101	198	66.22%
	73.77%	76.15%	

Overall Statistics

Overall Accuracy	Overall Error	Cohen's kappa (κ)	Correctly Classified	Incorrectly Classified
74.73%	25.27%	0.487	482	163

Extreme Gradient Boost

Confusion Matrix

	fair (Predicted)	fraud (Predicted)	
fair (Actual)	305	41	88.15%
fraud (Actual)	51	248	82.94%
	85.67%	85.81%	

Overall Statistics

Overall Accuracy	Overall Error	Cohen's kappa (κ)	Correctly Classified	Incorrectly Classified
85.74%	14.26%	0.713	553	92

Figure 8: KNIME's output of Confusion Matrices of four distinct classification models based on dataset B

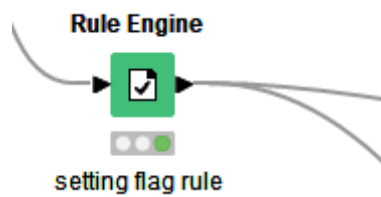


Figure 12: Rule engine for Flag Classification as either fraud or fair.

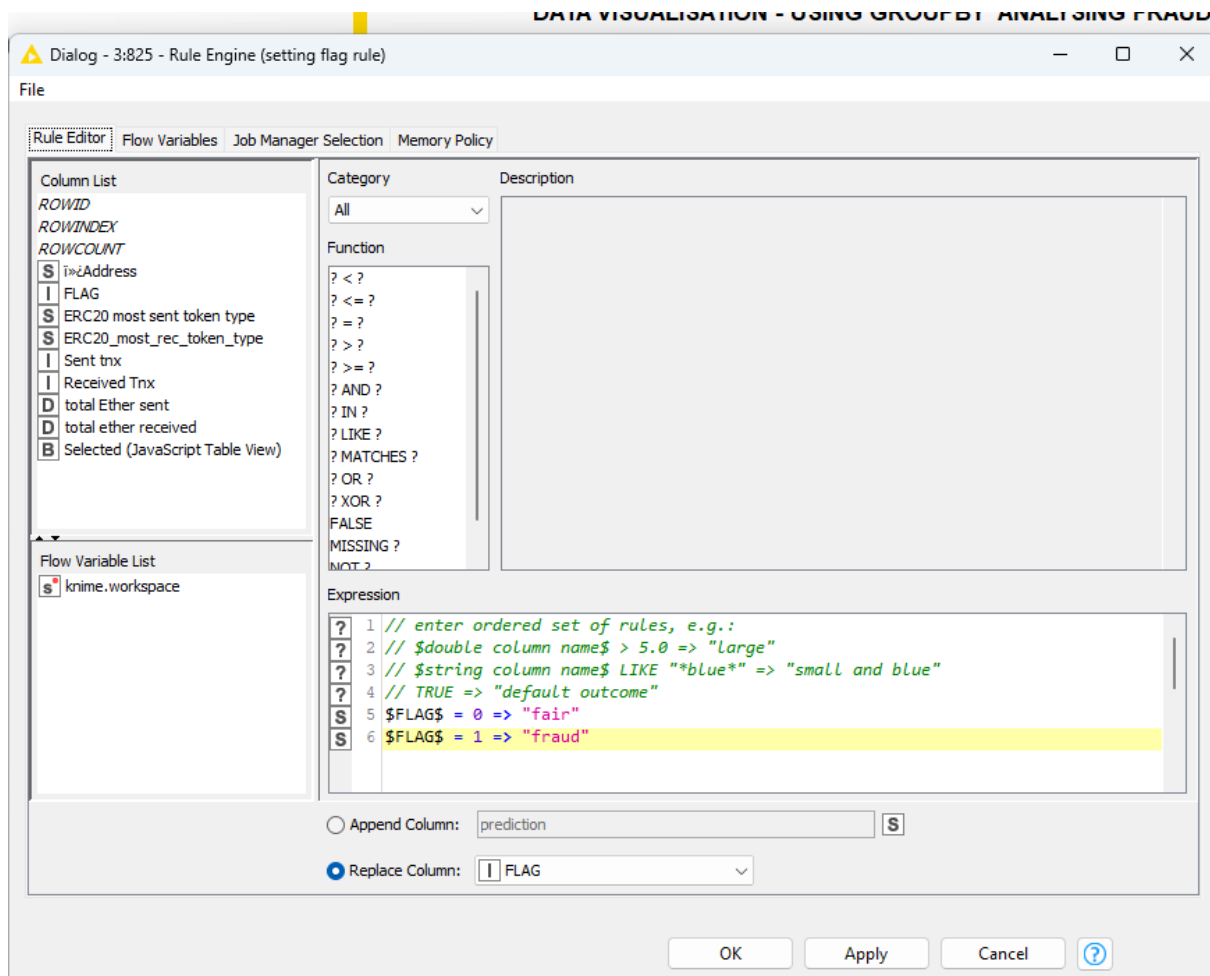


Figure 12: Rule engine's Expression for Flag Classification as either fraud or fair.

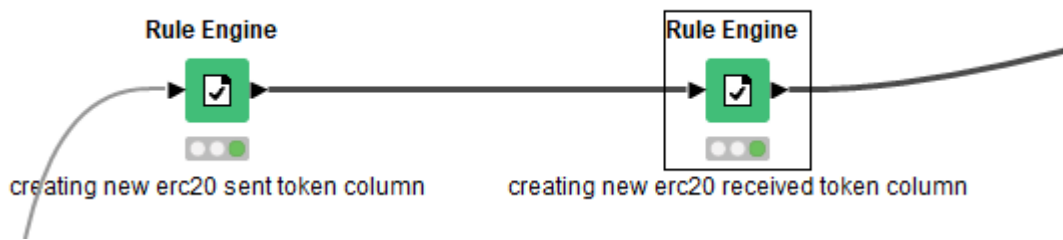


Figure 13: Rule engines for Classification of 612 tokens into 8 categories.

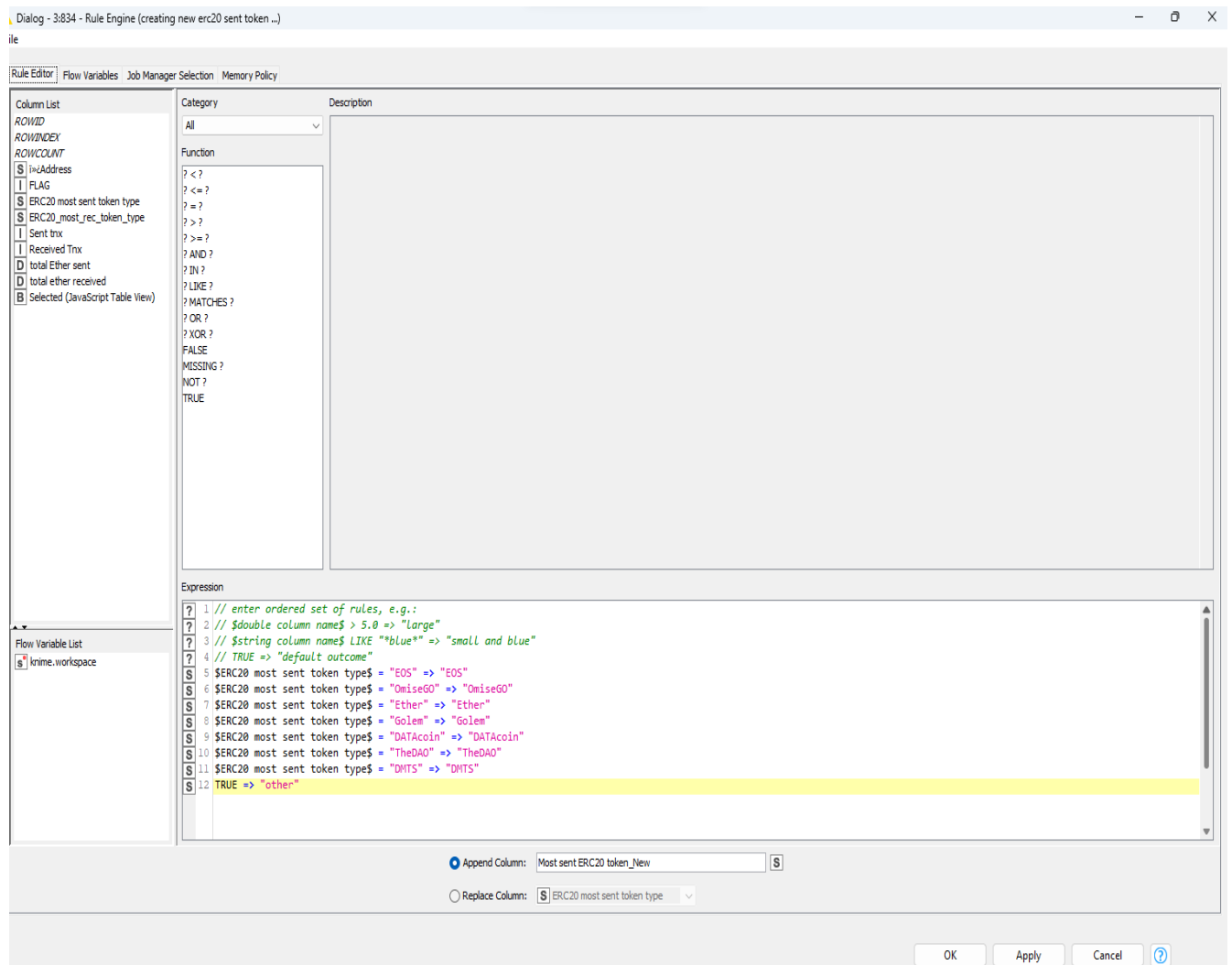


Figure 14: Rule engine's expression for ERC-20 sent tokens' classification for dataset B.

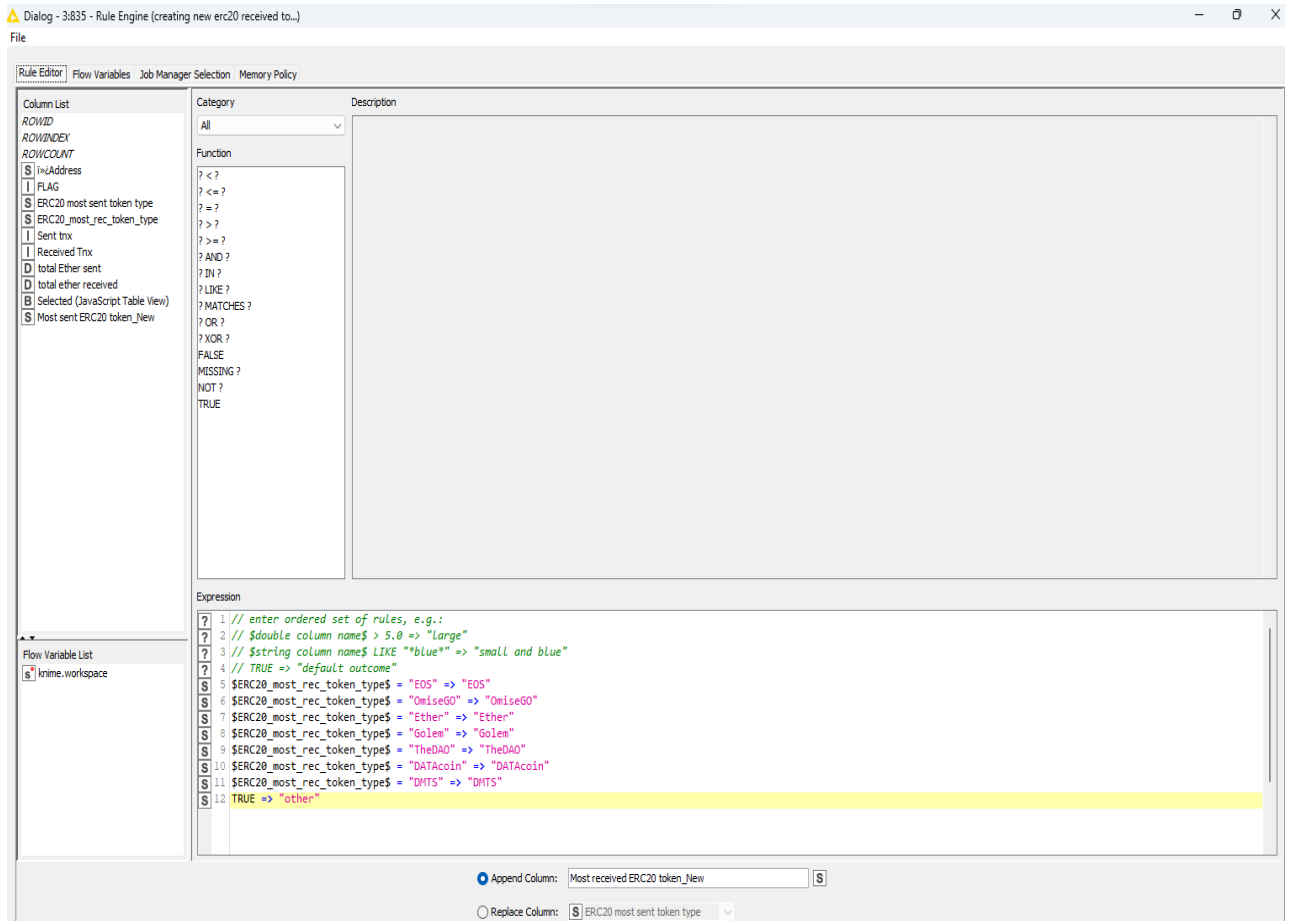


Figure 15: Rule engine's expression for ERC-20 received tokens' classification for dataset B.

6. References

- Antonopoulos, A.M. and Gavin Wood Ph.D (2018). *Mastering Ethereum*. O'Reilly Media.
- Barnett, Vic; Lewis, Lewis (1978). *Outliers in statistical data*. John Wiley & Sons Ltd.
- Berthold, M.R., Cebron, N., Dill, F., Gabriel, T.R., Kötter, T., Meinl, T., Ohl, P., Thiel, K. and Wiswedel, B. (2009). KNIME - the Konstanz information miner. *ACM SIGKDD Explorations Newsletter*, 11(1), p.26. doi:<https://doi.org/10.1145/1656274.1656280>.
- Bruce, P. and Bruce, A. (2017). *Practical Statistics for Data Scientists*. 'O'Reilly Media, Inc.'
- Chawla, N.V., Bowyer, K.W., Hall, L.O. and Kegelmeyer, W.P. (2002). SMOTE: Synthetic Minority Over-sampling Technique. *Journal of Artificial Intelligence Research*, 16(16), pp.321–357. doi:<https://doi.org/10.1613/jair.953>.
- Cohen, J. (1988). *Statistical Power Analysis for the Behavioral Sciences*. 2nd ed. Routledge. <https://doi.org/10.4324/9780203771587>.
- Farrugia, S., Ellul, J. and Azzopardi, G. (2020). Detection of illicit accounts over the Ethereum blockchain. *Expert Systems with Applications*, p.113318. <https://doi.org/10.1016/j.eswa.2020.113318>.
- Han, J., Kamber, M. and Pei, J. (2012). *Data mining: concepts and techniques*. Burlington, Ma: Elsevier.
- Hillemann, E.-C., Nussbaumer, A. and Albert, D. (2015). The Role of Cognitive Biases in Criminal Intelligence Analysis and Approaches for their Mitigation. *2015 European Intelligence and Security Informatics Conference*. <https://doi.org/10.1109/eisic.2015.9>.
- Reynolds, S. (2022). *Most Crypto Scams on BNB Chain, Solidus Labs Says*. [online] www.coindesk.com. Available at: <https://www.coindesk.com/business/2022/10/27/most-crypto-scams-on-bnb-chain-solidus-labs-says/> [Accessed 15 Mar. 2023].

Piryonesi, S.M. and El-Diraby, T.E. (2020). Data Analytics in Asset Management: Cost-Effective Prediction of the Pavement Condition Index. *Journal of Infrastructure Systems*, 26(1), p.04019036. [https://doi.org/10.1061/\(asce\)is.1943-555x.0000512](https://doi.org/10.1061/(asce)is.1943-555x.0000512).

Zhang, D., Qian, L., Mao, B., Huang, C., Huang, B. and Si, Y. (2018). A Data-Driven Design for Fault Detection of Wind Turbines Using Random Forests and XGboost. *IEEE Access*, 6, pp.21020–21031. <https://doi.org/10.1109/access.2018.2818678>.